Microstructural characterization of $YBa_2Cu_3O_{7-x}$

M. Sarikaya, B. L. Thiel, and I. A. Aksay
Department of Materials Science and Engineering, and Advanced Materials Technology Program, Washington Technology Center, University of Washington, Seattle, Washington 98195

W. J. Weber and W. S. Frydrych
Pacific Northwest Laboratory, Richland, Washington 99352

(Received 8 July 1987; accepted 24 August 1987)

A detailed characterization study on polycrystalline specimens of $YBa_2Cu_3O_{7-x}$ that were prepared by solid-state reaction techniques has been carried out. In the samples studied, magnetization and resistivity measurements indicate superconductivity onset temperatures of up to 89 K. Transmission electron microscopy (TEM) techniques have been used to facilitate direct microstructural characterization. It is shown that the planar defects on (001) planes form during the ion milling of the samples and are not directly connected with superconductivity. Laser Raman spectroscopy has revealed that these materials are sensitive to environmental degradation.

I. INTRODUCTION

Superconductivity above 30 K was first reported by Bednorz and Müller[1] in a La–Ba–Cu–O compound. A number of other related compounds were found that exhibited superconductivity with layered-like structural packing similar to K_2NiF_4.[2,8] Through improved sample preparation techniques,[3,5,9] changes in chemical constituents,[5] and applied pressure,[4] the transition temperature T_c was raised above 30 K, and the transition width was reduced. It is now possible to prepare nearly pure phase RE–Ba–Cu–O compounds (RE = Y, Nd, Sm, Eu, Gd, Ho, Er, and Lu) that show T_c between 90 and 95 K and that show bulk superconductivity.[5] The most recent studies indicate that the critical temperature has risen to 155 K in compounds where O is partially replaced by F[10] and to 240 K in compounds that contained the same atomic species as in the original Y–Ba–Cu–O samples but in different amounts.[11(a),(b)] However, neither the exact composition nor the crystal structure or other structural features of these new phases are yet known. As more experimental information is accumulated about these compounds, T_c may be expected to rise to even higher temperatures.

The reports made in the literature[3,5] and the results of diffraction and transmission electron microscopy (TEM) studies in our laboratory[12] indicate that the original high-T_c samples consisted of more than one phase. Subsequent studies have determined that the high-T_c superconductor can be produced in a single phase with a composition $YBa_2Cu_3O_{7-x}$.[13,14] These compounds have either tetragonal[5,15] or orthorhombic crystal structures,[3,6,9,12–14,16] as determined by x-ray and neutron diffraction. Although some models have been developed on the atomic packing of these crystals that are supported by theoretical and experimental studies through the bulk measurements,[3,6,16] these models have not all agreed with one another on the actual arrangements of the atoms and the relationships of atomic layers within the lattice. In some recent atomic resolution electron microscopy studies,[17(a)–(c)] not only was the lattice of the 90 K phase (pseudo-orthorhombic) successfully imaged, directly in (100) orientation revealing the position of the atomic species, but also some unexpected lattice defects were found. The effect of these defects on the superconductivity in these samples is not yet known. Only limited information has been reported in the literature on the micro- and nano-structural variations in polycrystalline high-T_c superconducting samples.

Presently, what is needed is the use of techniques that would (i) allow the revelation of the phase that produce superconductivity at high temperatures; (ii) that would provide information about their spatial distribution, crystal structure, and composition; and (iii) that would provide direct spectroscopic information. This article focuses on the morphology and crystallography of superconducting $YBa_2Cu_3O_{7-x}$ as studied by high-resolution TEM techniques. During the preparations, unprecedented modifications may be introduced to the thin sections used for TEM observations. This could lead to erroneous interpretations. Therefore the purpose of this report is twofold: first, to explain the techniques used in the preparation of electron transparent sections for TEM observations, and second, to perform microstructural and spectroscopic analyses of polycrystalline samples.

II. EXPERIMENTAL PROCEDURE

A. Sample preparation

Samples of $YBa_2Cu_3O_{7-x}$ were prepared for this study by the solid-state reaction of Y_2O_3, BaO_2, and

0003-6951/87/060736-07$01.75

CuO powders mixed in stoichiometric proportions. The powders were reacted at 900 °C for several hours in air; they were then crushed, remixed, and heated again at 925 °C for a more complete reaction to the single-phase $YBa_2Cu_3O_{7-x}$ composition. After another crushing, the powder was pressed at about 35 MPa into bars, sintered at 950 °C in air for 6 h, and slow cooled to room temperature. Further heat treating was not performed on the samples used in the studies reported here.

B. TEM specimen preparation

Two techniques were used for preparation of electron transparent sections for TEM observation: (i) ion milling and (ii) ultramicrotomy. In the first case, the regular preparation procedure was used in which thin slices (200 μm thick) from a bulk pellet were cut and mechanically thinned down to 50 μm. These were then cut into 2×2 mm disks that were mounted on oval Cu support grids with colloidal silver. Ion milling was performed with a dual gun ion miller under the following conditions: voltage—6 kV; beam current—0.4 mA; tilt angle—22°–22°; and milling time—6–8 h.

In the second procedure the sample was crushed into powder, which was then embedded in an epoxy (embedding was preferred over suspending particles on a carbon film to increase the stability of particles during electron bombardment). Thin sectioning was done by an ultramicrotome to obtain 30–80 nm thick slices. These slices of epoxy containing sectioned powders were then suspended onto 20 nm thick carbon film attached to a Cu grid.[18]

III. EXPERIMENTAL RESULTS AND DISCUSSION

A. Superconductivity

The superconducting nature of the samples used in the TEM studies below was confirmed by standard four-point resistivity measurements and by measurements of the magnetic flux expulsion in a weak ac field. The resistivity results in Fig. 1 indicate an onset temperature for superconductivity of 89 K for these samples. Similar behavior occurs for the flux expansion measurements, as shown in Fig. 2, which also indicates a superconducting volume fraction in these samples of about 75% at 77 K. Higher volume fractions of superconductivity, as determined by flux expulsion measurements, have been obtained by an additional heat treatment in oxygen at 450 °C. These materials are currently undergoing extensive spectroscopic characterization, and the results will be reported at a later date.

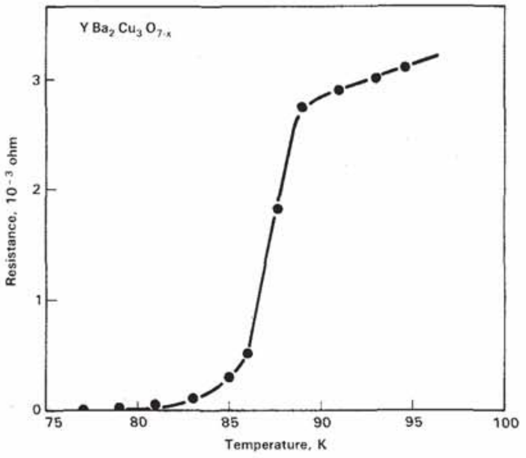

FIG. 1. Superconducting transition measured by four-point resistance measurements.

B. Effect of thin section preparation

Thin sections prepared by using the two techniques described above exhibited grossly differing microstructures because of the modifications induced during preparation. In Figs. 3(a) and 3(b), images [in (010) orientation] from the ultramicrotomed and ion-milled specimens, respectively, are shown. In the superconducting phase of the ion-milled sample, there are planar defects with sizes 2–10 nm in thickness and 20–100 nm in length. These defects lie on (001) planes and were induced during the ion milling. The presence of these externally induced defects, which are not present in the ultramicrotomed samples, has erroneously been associated with the superconductivity seen in these materials in the literature.[17(a)] These defects have persisted even with low-temperature holders (liquid nitrogen stage) and they constituted more than 50% of the superconducting phase. The results presented below were obtained by carefully selecting nondefective regions in

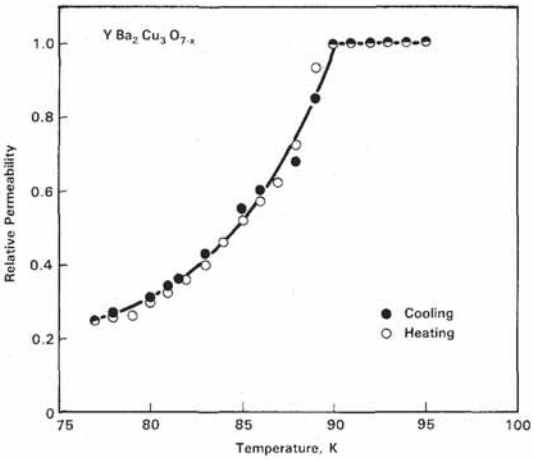

FIG. 2. Magnetic flux expulsion as a result of superconducting transition.

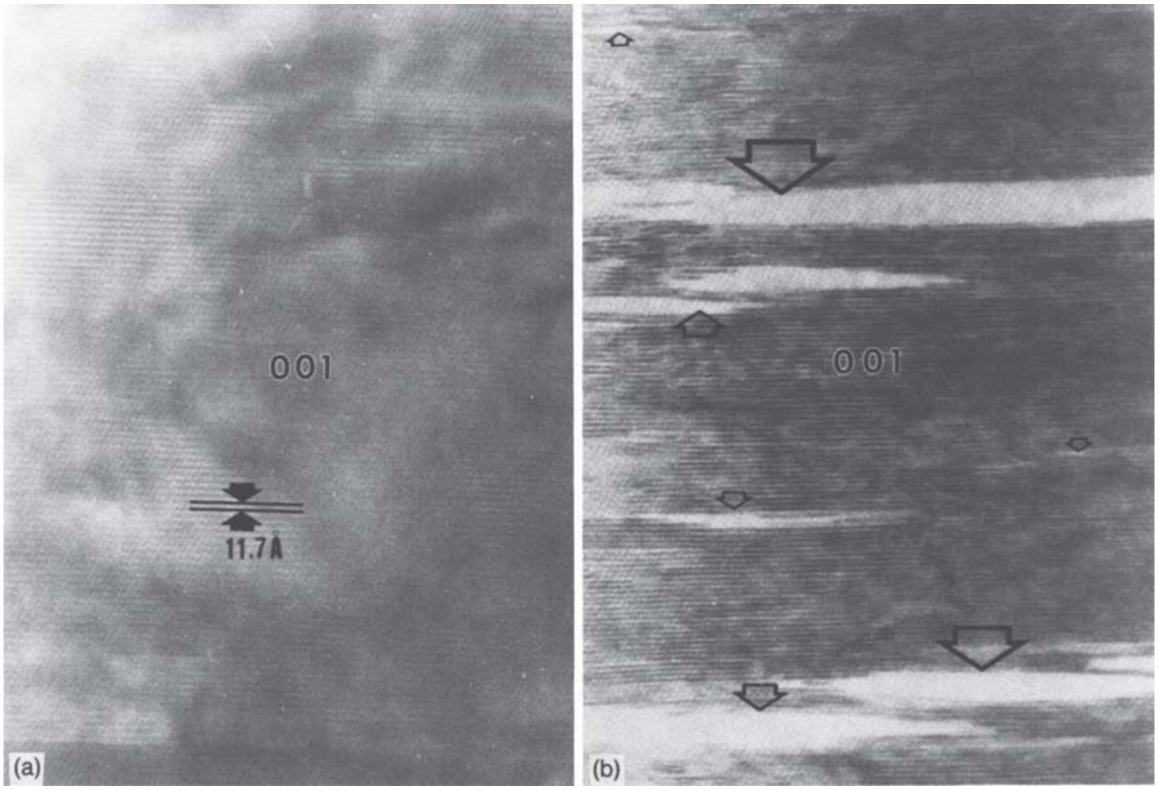

FIG. 3. The TEM micrographs revealing (a) no damage in a foil prepared by ultramicrotomy and (b) damage in a foil prepared by ion milling. Note the (001) fringes in both cases.

the ion-milled samples and by using ultramicrotomed sections.

C. Crystal structure determination

Although some controversy exists in the literature over the exact nature of the crystal structure of the superconducting phase with composition $YBa_2Cu_3O_{7-x}$, the same pseudo-orthorhombic structure persisted in samples used in this study, as examined by x-ray and electron diffraction techniques.[12] We have observed degradation of the superconductivity (flux expulsion and flux exclusion) as a result of exposure to water or long exposure to atmospheric humidity. Presently, it is not known whether this is due to the changes that may take place in the composition, in the crystal structure, and in the substructure (e.g., relaxation of twins,[12] or ordering of vacancies), or in combinations of these. In this study x-ray and electron diffraction studies were performed in order to determine if there is any effect on the crystal structure and the lattice parameters. Within the limits of the x-ray diffraction (XRD) measurements, no detectable change was observed in the lattice parameters of the pseudo-orthorhombic phase. This was also true in electron diffraction studies. However, results from laser Raman spectroscopy on a freshly fractured surface of $YBa_2Cu_3O_{7-x}$ at room temperature revealed changes in the metal/oxygen stretching region of the spectrum as a function of exposure time to laboratory atomsphere. This behavior, shown in Fig. 4, suggests alteration of the molecular structure at the surface, which apparently is not detectable by x-ray or electron diffraction. Further studies of environmental degradation are in progress.

A representative result of a controlled tilting experiment is presented in Fig. 5, where eight zone axis electron microdiffraction patterns are shown that were recorded along two mutually orthogonal Kikuchi line pairs. Low symmetry axes were chosen to enhance any change in the crystallographic properties. The measurements made in the interplanar spacing and the angles between the poles indicate that they are in agreement with the original pseudo-orthorhombic structure with the lattice parameters $a = 0.3826$ nm, $b = 0.3891$ nm, and $c = 1.1695$ nm.[12]

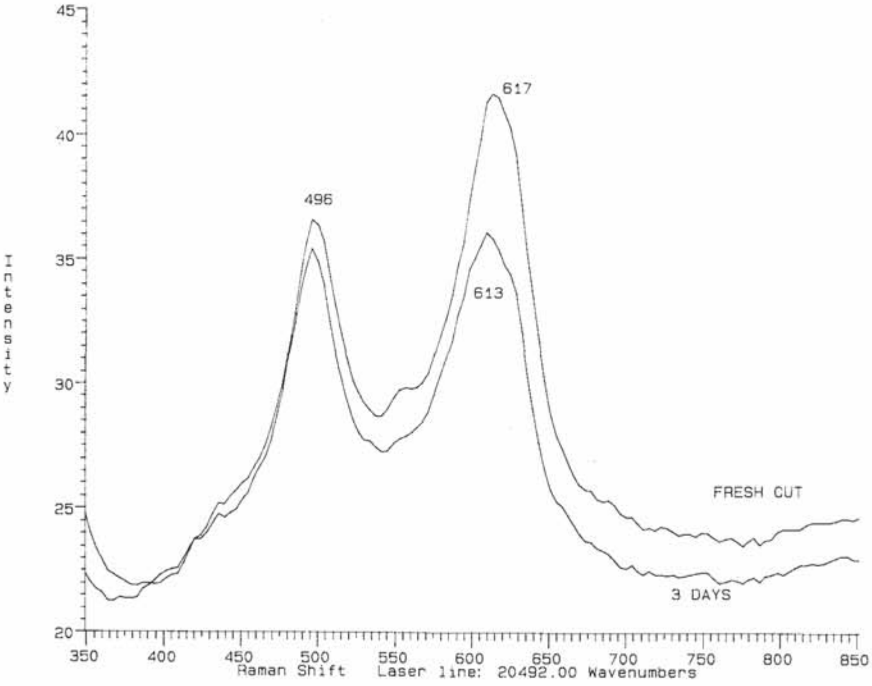

FIG. 4. Raman spectra of freshly fractured $YBa_2Cu_3O_{7-x}$ as a function of time.

D. Submicrostructural analysis

As reported earlier, the grains having the pseudo-orthorhombic crystal structure are in the form of laths with varying thickness 2–5 μm, height 2–10 μm, and length 5–30 μm.[12] Fine twins were observed in these grains that have (110) twin planes. The thickness of the twin crystals changed depending on the size of the original grain. Also, in large grains both the (110) and the $(1\bar{1}0)$ variants of the twins were observed.[12] An analysis of the twins is presented in Fig. 6, which includes the dark-field (DF) images taken from the twin and the matrix [(b) and (c), respectively]. A diffraction pattern that was recorded in [001] zone axis orientation with a large camera length is shown in Fig. 6(a). The analysis of twinning is shown in Fig. 6(f), which reveals spot splitting due to twinning and the difference in *a* and *b* lattice parameters, which is about 2%. It should be noted that in recording the dark-field images, third-order reflections were used where the splitting is about 5 mrad, in order to exclude the contribution of each of the reflections to the image of the other.

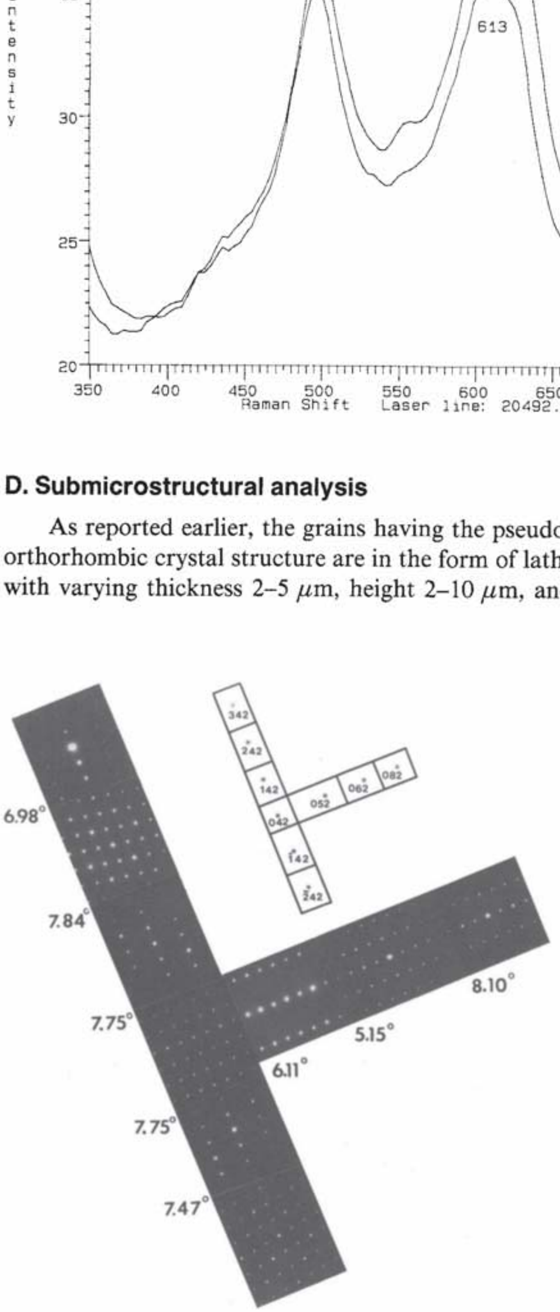

FIG. 5. Result of a representative tilting experiment. The indices of the poles corresponding to the zone axis patterns and the angles between these poles are indicated.

A close observation of the DF images in Figs. 6(b) and 6(c) reveals that a thin lath shaped matrix and twinned crystals with a fairly uniform thickness extend along the length of the grains and that thicker occasional matrix crystals contain "subtwins." The size of the twins and the presence of subtwins indicate that large stresses must have been accommodated during the formation of the pseudo-orthorhombic phase that may have formed as a result of a martensitic transformation. This result is consistent with the formation of substructural twins in high carbon steels. In this case, as the carbon content of austenite (the high-temperature phase) increases and the lattice is more constrained, during the transformation the number of twins increases

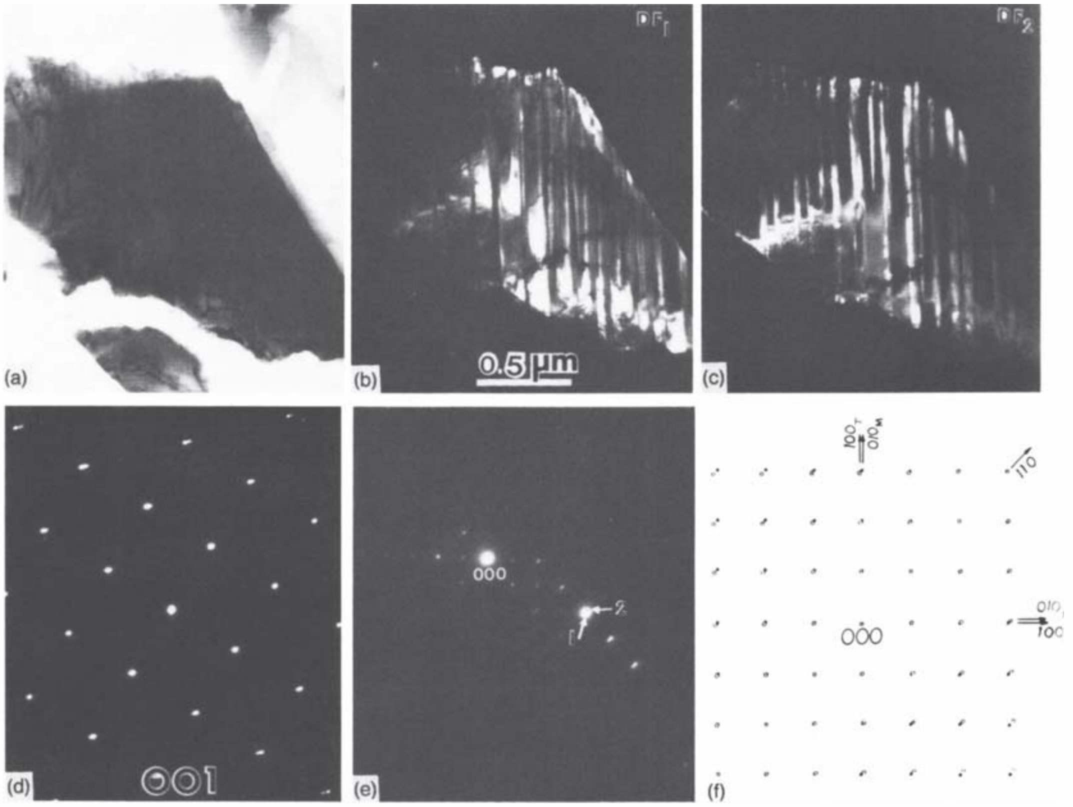

FIG. 6. Analysis of substructural twins in the pseudo-orthorhombic structure. (a) Bright-field and (b) and (c) dark-field images, taken by using the third-order reflections shown in (e). Here (d) is a selected area diffraction pattern and (f) is the analysis of (110) twin.

concurrent with a decrease in the average thickness of the twins in the martensitic ferrite (low-temperature phase).[19]

E. Electron-beam damage

The spectroscopic techniques accessible in the TEM make use of small electron probes. These techniques are energy dispersive x-ray spectroscopy and electron energy loss spectroscopy that are, respectively, used most often to determine elemental composition and chemical and electronic states of the elements. Probe diameters that are used change depending on the count rate that is produced in a particular area. It is often necessary to use a large probe size to obtain good statistics. However, there is a danger of radiation damage due to heating and knock-on that cause a change in the local composition and/or chemical state.

Experiments were performed to elucidate the effect of electron-beam damage on the superconducting phase. As exemplified in Fig. 7, electron-beam damage can be introduced (under extreme operating conditions) to the superconducting phase. The images and the diffraction patterns shown in Fig. 7 were taken before and after 5 min exposure. The analysis of the ring diffraction pattern in Fig. 7(d) indicated that the islands in Fig. 7(c), which form after the damage, were precipitates of elemental copper. The (001) fringes could still be seen in the same image; they are discontinuous because of the damage created in the matrix that also eliminates the twins.

IV. SUMMARY AND CONCLUSIONS

Transmission electron microscopy is a powerful tool that combines many techniques in identifying microstructural, compositional, and crystallographic features at high spatial resolutions, especially in complex polycrystalline multiphase samples. However, extreme caution has to be taken, as demonstrated in this article, in using standard techniques in the preparation of thin foils from unfamiliar samples and degradations induced by radiation damage during the observation of these foils.

It is shown that planar defects form on (001) planes during the ion milling of the samples. In previous studies[17] these defects were erroneously attributed as having

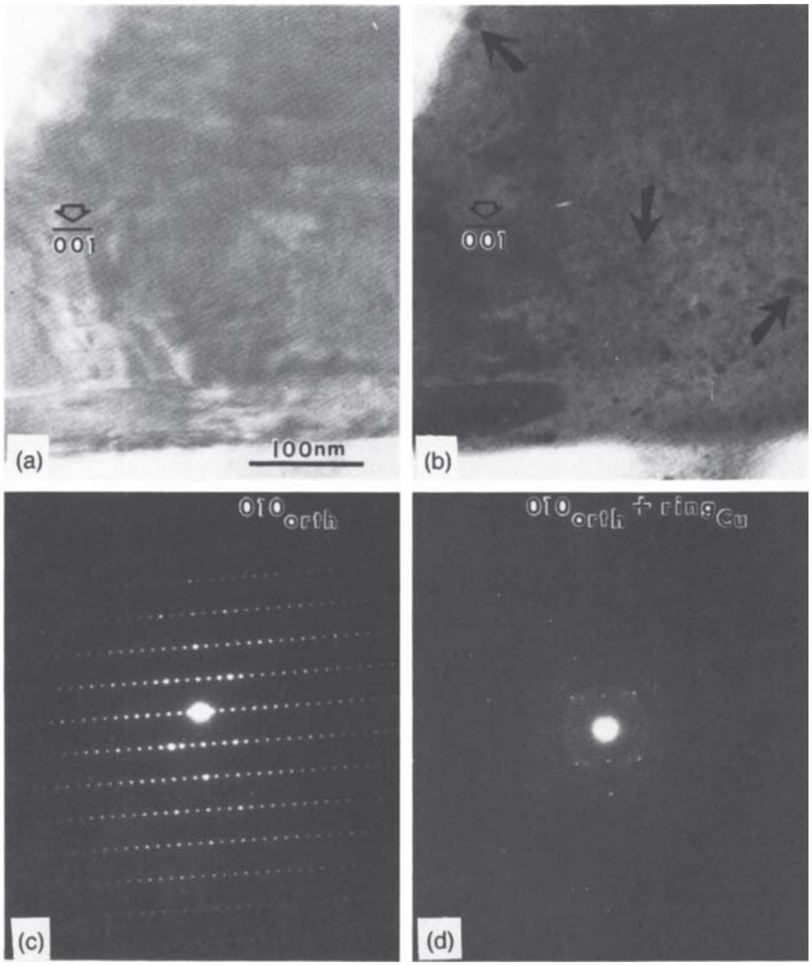

FIG. 7. Radiation damage experiment (a) before and (b) after the radiation. Diffraction pattern in (c) reveals only (010) orthorhombic pattern and (d) reveals both (010) orthorhombic pattern and a ring pattern from elemental Cu. In (a) and (b) (001) lattice planes are resolved. The arrows indicate Cu "islands" (E_0, 300 keV; C2 aperture out; fully condensed beam).

connections with superconductivity. It is also illustrated that radiation damage, under extreme conditions of observation, can cause the reduction of Cu in the $YBa_2Cu_3O_{7-x}$ phase. There is also a slight possibility that the substructural twins may be induced during mechanical polishing since such effects have been seen in the preparation of other ceramic samples (such as in zirconia).[20] Fortunately, if the necessary steps are taken, these unprecedented modifications to the samples can be eliminated.

Although specimens lose their superconducting behavior under normal atmospheric conditions, there have not been any crystallographic differences observed either by XRD or electron diffraction studies. However, preliminary experiments using Raman spectroscopy indicated changes in Cu–O stretching in fractured specimens during the exposure to atmosphere. Further studies are underway to elucidate the environmental effects on the crystallographic (changes in the symmetry operators due to possible changes in the O occupancy), compositional, and spectroscopic characteristics of the samples.

It should be emphasized here, provided that necessary precautions are taken in foil preparation and observation, that with the use of an atomic resolution imaging technique combined with the use of small electron probes (5.0 nm) in acquiring crystallographic and spectroscopic information, transmission electron microscopy will be extremely useful in performing phase transformations and phase equilibria studies in complex oxides that exhibit high-temperature superconductivity.

ACKNOWLEDGMENTS

The University of Washington portion of this work was sponsored by the Air Force Office of Scientific Research (AFOSR) and the Defense Advanced Research Projects Agency (DARPA) and was monitored by

AFOSR under Grant No. AFOSR-87-0114. The Pacific Northwest Laboratory work was supported by the United States Department of Energy, Office of Basic Energy Sciences under Contract No. DE-AC06-76RLO 1830.

REFERENCES

[1] J. G. Bednorz and K. A. Müller, Z. Phys. B **64**, 189 (1986).

[2] C. W. Chu, P. H. Hor, R. L. Meng, L. Gao, Z. U. Huang, and Y. Q. Wang, Phys. Rev. Lett. **58**, 405 (1987).

[3] R. J. Cava, R. B. van Dover, B. Batlogg, and E. A. Reitman, Phys. Rev. Lett. **58**, 408 (1987).

[4] M. K. Wu, J. R. Ashburn, and C. J. Torng, Phys. Rev. Lett. **58**, 908 (1987).

[5] P. H. Hor,L. Gao, R. L. Meng, Z. J. Hunag, Y. Q. Wang, K. Forster, T. Vassillious, and C. W. Chu, Phys. Rev. Lett. **58**, 911 (1987).

[6] M. A. Beno, L. Soderholm, D. W. Capone, II, D. G. Hinks, J. D. Jorgensen, I. K. Schuller, C. A. Seegre, K. Zhang, and J. D. Grace, Appl. Phys. Lett. **51**, 57 (1987).

[7] M. Hirabayashi, H. Ihara, N. Terada, K. Senzaki, K. Hayashi, S. Waki, K. Murata, M. Tokumoto, and Y. Kimura, Jpn. J. Appl. Phys. **26**, L454 (1987).

[8] J. D. Jorgensen, H.-B. Schüttler, D. G. Hinks, D. W. Capone, II, K. Zhang, and M. B. Brodsky, Phys. Rev. Lett. **58**, 1024 (1987).

[9] J. Z. Liu, G. W. Crabtree, A. Umezawa, and Li Zongquan, Phys. Lett. A **123**, 305 (1987).

[10] S. R. Ovshinsky, R. T. Young, D. D. Allred, G. DeMaggio, and G. A. Van der Leeden, Phys. Rev. Lett. **58**, 2579 (1987).

[11] J. T. Chen, L. E. Wenger, C. J. McEwan, and E. M. Logothetis, edited by V. Kresin and S. Wolf (Pelnum, New York, 1987); A. Zettl and C. W. Chu, in *The Proceedings of the International Conference on Novel Mechanism of Superconductivity*, Berkeley, California, 22–26 June 1987, edited by V. Kresin (Pergamon, New York, 1987).

[12] W. J. Weber, L. R. Pederson, J. M. Prince, K. C. Davis, G. J. Exurhos, G. D. Maupin, J. T. Prater, W. S. Frydrych, I. A. Aksay, B. L. Thiel, and M. Sarikaya, Adv. Ceram. Mater. **2** (3B), 471 (1987).

[13] I. K. Schuller, D. G. Hinks, M. A. Beno, D. W. Capone, II, L. Soderholm, J.-P. Locquet, Y. Bruynseraede, C. U. Segre, and K. Zhang, Solid State Commun. **63**, 385 (1987).

[14] D. G. Hinks, L. Soderholm, D. W. Capone, II, J. D. Jorgensen, I. K. Schuller, C. U. Sagre, K. Zhang, and J. D. Grace, Appl. Phys. Lett. **50**, 1688 (1987).

[15] T. Hatano, A. Matsushita, K. Nakamura, K. Honda, T. Matsumoto, and K. Ogawa, Jpn. J. Appl. Phys. **26**, L374 (1987).

[16] E. Takayama-Muromachi, Y. Uchida, Y. Matsui, and K. Kato, Jpn. J. Appl. Phys. **26**, L476 (1987).

[17] (a) A. Ourmazd, J. A. Rentschler, J. C. H. Spence, M. O'Keeffe, R. J. Graham, D. W. Johnson, Jr., and W. W. Rhodes, Nature **327**, 308 (1987); (b) E. A. Hewat, M. Dupuy, A. Bourret, J. J. Capponi, and M. Marezio, Nature **327**, 400 (1987); (c) R. Gronsky (private communication).

[18] J. P. Bradley and D. E. Brownlee, Science **231**, 1542 (1986).

[19] Z. Nishiyama, *Martensitic Transformations* (Academic, New York, 1978).

[20] A. G. Evans and A. H. Heuer, J. Am. Ceram. Soc. **63**, 241 (1980).